JOURNAL OF COMPUTATIONAL PHYSICS **128,** 351–362 (1996)
ARTICLE NO. 0216

Numerical Study of a Stochastic Weighted Particle Method for a Model Kinetic Equation

SERGEJ RJASANOW* AND WOLFGANG WAGNER†

*Department of Mathematics, University of Kaiserslautern, Postfach 3049, D-67653 Kaiserslautern, Germany; †Weierstrass Institute for Applied Analysis and Stochastics, Mohrenstrasse 39, D-10117 Berlin, Germany

Received February 21, 1996

A stochastic weighted particle method is applied to a model nonlinear kinetic equation. A detailed study of various numerical approximations is presented. The main effect achieved by the new method is an artificial increase of the relative number of simulation particles with prescribed velocities.

1. INTRODUCTION

In this paper we continue the study of a new particle method for nonlinear kinetic equations introduced in [8]. This method is based on a generalized procedure of modelling collisions between particles providing some freedom in the random choice of the collision partners and in the weight transfer mechanism (cf. [5, 4, 9].)

We consider the equation

$$\frac{\partial}{\partial t} f(t,u) = \int_0^1 [f(t,u-v)f(t,v) - f(t,u)f(t,v)]\, dv, \quad (1.1)$$

where $t > 0$, $0 \le u < 1$, with the initial condition

$$f(0,u) = f_0(u). \quad (1.2)$$

The solution $f(t, u)$ is assumed to be periodic in u, i.e.,

$$f(t,u) = f(t,1+u), \quad t \ge 0, u \in \mathbb{R}.$$

Equation (1.1) is a model kinetic equation, which is nonlinear but has a very simple collision mechanism. The simplicity of this equation allows us to check all steps of the numerical algorithm very carefully in order to give recommendations for more complicated kinetic equations, like the Boltzmann equation (cf. [3]). In [9], where also the convergence of the method was investigated, we used Eq. (1.1) to illustrate the reduction of the statistical fluctuations.

A challenging problem related to the Boltzmann equation is the accurate calculation of macroscopic quantities, like mean velocity or temperature, in regions with a small particle density. This problem can hardly be solved efficiently by direct simulation methods in such cases, where the changes of the particle density are of several orders of magnitude. We refer to [1; 3, Chap. 10; 6; 7] concerning particle schemes for the Boltzmann equation.

In simulation procedures for the spatially inhomogeneous Boltzmann equation (cf., e.g., [8]), a time discretization

$$t_k = k\,\Delta t, \quad k = 0, 1, ..., \Delta t > 0,$$

is used in order to split the simulation of the free flow of the particles and the simulation of their collisions. This means that on a small time interval of length Δt, at a first step, the free flow is simulated, disregarding the possible collisions. Then, at a second step, the collisions are simulated, neglecting the free flow. Now, if one wishes to increase artificially the number of simulation particles in a certain region of the physical space, then it will be necessary to generate particles with velocities from a prescribed subset of the velocity space during the collision simulation step.

The main objective of this paper is to show that this goal, i.e., an artificial increase of the number of particles with prescribed velocities, can be achieved by the new method. We also study the related effect of variance reduction, the influence of various approximation procedures for the initial distribution, and the effect of different time counting mechanisms on the simulation results.

The paper is organized as follows. In Section 2, we summarize the main analytical properties of the model equation and give an appropriate exact solution for the numerical tests. In Section 3, we describe the stochastic weighted particle method. In Section 4, we illustrate the various numerical effects mentioned above. Finally, we draw some conclusions.

2. ANALYTICAL PROPERTIES OF THE EQUATION

The model kinetic equation (1.1) was introduced in [2], where the existence of the solution, as well as its stability

0021-9991/96 $18.00

and the convergence of a class of difference schemes was studied. In particular, it was proved that the solution of the initial value problem (1.1), (1.2) exists in $L_2([0, 1))$ for $t \geq 0$ and any initial function $f_0 \in L_2([0, 1))$.

The solution can be represented in terms of Fourier series

$$f(t, u) = \sum_{k \in \mathbb{Z}} \frac{\varrho c_k(0)}{c_k(0) - (c_k(0) - \varrho) e^{\varrho t}} v_k(u),$$

where

$$v_k(u) = e^{i 2\pi k u} \tag{2.1}$$

are the Fourier functions and i denotes the imaginary unit, i.e., $i^2 = -1$. The symbols $c_k(0)$ are the corresponding Fourier coefficents of the initial function f_0, i.e.,

$$f_0(u) = \sum_{k \in \mathbb{Z}} c_k(0) v_k(u).$$

The value ϱ is equal to the "mass" of the system and remains conserved by Eq. (1.1):

$$\varrho = \int_0^1 f(t, u)\, du = \int_0^1 f_0(u)\, du. \tag{2.2}$$

The L_2-norm of the solution $f(t, u)$ is estimated as

$$\|f(t, u)\|^2_{L_2([0,1))} = \sum_{k \in \mathbb{Z}} |c_k(t)|^2 \leq \sum_{k \in \mathbb{Z}} |c_k(0)|^2 = \|f_0(u)\|^2_{L_2([0,1))}.$$

For some special f_0, it is possible to give the analytical solutions of the problem (1.1) in terms of elementary functions. One of these solutions is obtained for the initial function

$$f_0(u) = 2 + \sin(2\pi u), \tag{2.3}$$

which can be written as

$$f_0(u) = -\frac{1}{2i} v_{-1}(u) + 2v_0(u) + \frac{1}{2i} v_1(u),$$

where $v_k(u)$ are defined in (2.1). The corresponding analytical solution is

$$f(t, u) = 2 + \frac{4(1 - e^{2t}) \cos(2\pi u) + 16 e^{2t} \sin(2\pi u)}{1 - 2e^{2t} + 17 e^{4t}}. \tag{2.4}$$

The moments of the solution (2.4)

$$M_k(t) = \int_0^1 u^k f(t, u)\, du, \quad k = 0, 1, ..., \tag{2.5}$$

can be computed explicitly. One obtains

$$M_k(t) = 2 + \frac{4(1 - e^{2t}) c_k + 16 e^{2t} s_k}{1 - 2e^{2t} + 17 e^{4t}}, \quad k = 0, 1, ..., \tag{2.6}$$

where

$$c_k = \int_0^1 u^k \cos(2\pi u)\, du, \quad s_k = \int_0^1 u^k \sin(2\pi u)\, du. \tag{2.7}$$

The numbers c_k and s_k are computed via the recursive formulae

$$c_0 = s_0 = 0, \tag{2.8}$$

$$c_k = -\frac{k}{2\pi} s_{k-1}, \quad s_k = -\frac{1}{2\pi} + \frac{k}{2\pi} c_{k-1}, \quad k = 1, 2, ... \tag{2.9}$$

Furthermore, we introduce the function

$$F_\varepsilon(t) = \int_{1-\varepsilon}^1 f(t, u)\, du, \quad \varepsilon > 0, \tag{2.10}$$

which takes the explicit form

$$F_\varepsilon(t) = 2\varepsilon + \frac{2((1 - e^{2t}) \sin(2\pi\varepsilon) - 4e^{2t}(1 - \cos(2\pi\varepsilon)))}{\pi(1 - 2e^{2t} + 17 e^{4t})}. \tag{2.11}$$

3. THE METHOD

The method consists in modelling trajectories of a stochastic particle system of the form

$$Z(t) = \{(w_i(t), g_i(t)), \quad i = 1, ..., m(t)\}, \quad t \geq 0. \tag{3.1}$$

Each particle has a state ("velocity") $w_i(t)$ from the interval [0, 1), and a weight $g_i(t) \in [0, 1]$. The variable $m(t)$ denotes the number of particles in the system, and

$$m(0) = n. \tag{3.2}$$

The justification of the method is given in [9] by showing convergence (as $n \to \infty$) of the corresponding empirical measures,

$$\mu(t, dw) = \sum_{i=1}^{m(t)} g_i(t)\, \delta_{w_i(t)}(dw), \tag{3.3}$$

where δ denotes the Dirac measure, to the measures $f(t, w)\, dw$, where f is the solution of Eq. (1.1).

3.1. *Approximation of the Initial Value*

The first step in the construction of the particle system (3.1) is the approximation of the initial function f_0 given in (2.3) by a system of particles

$$Z(0) = \{(w_i, g_i), i = 1, ..., n\}.$$

A natural choice of the weights at the beginning is

$$g_i = \frac{\varrho}{n}, \quad i = 1, ..., n, \tag{3.4}$$

where ϱ is defined in (2.2).

The problem of generating velocities w_i reduces to the numerical solution of the equations

$$\frac{1}{\varrho}\int_0^{w_i} f_0(u)\, du = r_i, \quad i = 1, ..., n, \tag{3.5}$$

where r_i are pseudo-random numbers. One can also choose the elements of a low discrepancy sequence for r_i (cf. [7]). According to (2.3), Eq. (3.5) takes the form

$$w_i - \frac{1}{4\pi}\cos 2\pi w_i = r_i - \frac{1}{4\pi}, \quad i = 1, ..., n,$$

and can be solved by the Newton method

$$w_i^{k+1} = \frac{2\pi \sin(2\pi w_i^k) + \cos(2\pi w_i^k) + 4\pi r_i - 1}{2\pi(2 + \sin(2\pi w_i^k)},$$

$$k = 0, 1, ...$$

A more general approach is first to divide the interval $[0, 1)$ into n_I parts using the nodes v_j, $j = 1, ..., n_I + 1$, defined from the equations

$$v_1 = 0, \quad \int_{v_j}^{v_{j+1}} f_0(u)\, du = \frac{\varrho}{n_I}, \quad j = 1, ..., n_I; \quad v_{n_I+1} = 1.$$

In each subinterval $[v_j, v_{j+1}]$, $j = 1, ..., n_I$, we put n/n_I particles according to the formulas

$$\frac{n_I}{\varrho}\int_{v_j}^{w_{j,i}} f_0(u)\, du = r_{j,i}, \quad j = 1, ..., n_I; i = 1, ..., n/n_I, \tag{3.6}$$

where $r_{j,i}$ are pseudo-random numbers. As in (3.5) it is also possible to use a low discrepancy sequence instead of pseudo-random numbers.

Another idea, which was used in [9], is to introduce particles having different weights already for the approximation of f_0.

3.2. *Time Evolution*

The evolution of the system (3.1) on a time interval $[0, \Delta t]$ is determined by discrete events, in each of which two particles are involved. Let

$$Z(t) = ((w_1, g_1), ..., (w_m, g_m)). \tag{3.7}$$

Then the principal steps of the procedure of modelling a transition

$$Z(t) \to Z(t + \tau)$$

are:

1. Increase the time counter $t := t + \tau$;
2. Choose the indices i and j of the collision partners;
3. Decide whether the collision is fictitious, i.e.,

$$Z(t + \tau) = Z(t);$$

4. If the collision is real, then perform the transformation

$$Z(t + \tau)_k = \begin{cases} (w_k, g_k), & \text{if } k \le m, k \ne i, j, \\ (\tilde{w}_i, G), & \text{if } k = i, \\ (\tilde{w}_j, G), & \text{if } k = j, \\ (w_i, g_i - G), & \text{if } k = m + 1, \\ (w_j, g_j - G), & \text{if } k = m + 2; \end{cases} \tag{3.8}$$

5. Decide whether some particles should be removed from the system because of their zero weights and define herewith the new number of particles $m(t + \tau)$.

The values $\tilde{w}_i$ and $\tilde{w}_j$ of the postcollision velocities are defined by the following collision transformation of velocities

$$\tilde{w}_i = \tilde{w}_j = w_i + w_j - [w_i + w_j], \tag{3.9}$$

where $[x]$ denotes the integer part of the value x.

The main parameter of the method is the **weight transfer function** G. This function should satisfy the inequality

$$0 \le G \le \min(g_i, g_j)$$

in order to keep the weights nonnegative.

We now describe a special choice of G, which is designed to increase the relative amount of particles in a special (small) region A_ε of the velocity space. This method is also capable of handling the problem of computing small

probabilities, i.e., of evaluating the function $F_\varepsilon(t)$ defined in (2.10). In this case, an appropriate choice is

$$A_\varepsilon = [1-\varepsilon, 1), \quad \varepsilon \in [0,1]. \tag{3.10}$$

The basic ideas are the following. First, if a particle reaches the interesting region A_ε then a part of it will always remain there, because in this case we will choose the weight transfer function

$$G = \frac{1}{1+\kappa_1}\min(g_i, g_j), \quad \kappa_1 > 0.$$

Second, with the help of another parameter κ_2 we will prefer collisions with postcollision velocities from the region A_ε in order to "encourage" the particles to enter this region.

Rigorously, the weight transfer function is defined as

$$G = \frac{1}{1+\gamma}\min(g_i, g_j), \tag{3.11}$$

where (cf. (3.7), (3.10), (3.9))

$$\gamma = \begin{cases} \kappa_1, & \text{if } w_i \in A_\varepsilon \text{ or } w_j \in A_\varepsilon, \\ \kappa_2, & \text{if } w_i, w_j \notin A_\varepsilon, \tilde{w}_i, \tilde{w}_j \in A_\varepsilon, \\ 0, & \text{otherwise.} \end{cases} \tag{3.12}$$

We consider two variants of defining the time step τ. On the one hand, the time step is determined by the deterministic term

$$\hat{\sigma} = \frac{2}{[1+\max(\kappa_1,\kappa_2)](m-1)(2\varrho - m g_{\min})}. \tag{3.13}$$

The value $g_{\min}$ denotes the minimal weight of all particles in the system $Z(t)$ and should be controlled and, if necessary, adapted after each collision. The value ϱ is defined in (2.2).

Alternatively, the time step is computed as a random variable σ having an exponential distribution with the parameter $\hat{\sigma}^{-1}$, i.e.,

$$\sigma = -\hat{\sigma}\log(r), \tag{3.14}$$

where r is a pseudo-random number. Note that the mathematical expectation of the random variable σ is just $\hat{\sigma}$. In the limit of large m, both alternatives are equivalent.

The indices i and j are generated as follows. First, the index i is chosen according to the probabilities

$$p_i = \frac{(m-2)g_i + \varrho - (m-1)g_{\min}}{(m-1)(2\varrho - m g_{\min})}. \tag{3.15}$$

Then, given the value of i, the index j is chosen according to the probabilities

$$p_j = \frac{g_i + g_j - g_{\min}}{(m-2)g_i + \varrho - (m-1)g_{\min}}. \tag{3.16}$$

The choice of the indices i and j can be performed by von Neumann's acceptance–rejection method.

The collision is fictitious with probability

$$\overline{p} = 1 - \frac{1+\gamma}{1+\max(\kappa_1,\kappa_2)}\frac{\max(g_i, g_j)}{(g_i + g_j - g_{\min})}, \tag{3.17}$$

where γ is defined in (3.12).

The number of particles increases by two in the case $\gamma > 0$. In the case $\gamma = 0$, it does not change, if the weights g_i and g_j are equal, or increases by one, otherwise.

3.3. *Comments*

The simplest variant of the method is obtained in the case $\kappa_1 = \kappa_2 = 0$, where we have (cf. (3.12), (3.11), (3.4), (3.13), (3.15), (3.16))

$$G = \varrho/n, \quad \tau = \frac{2}{\varrho(n-1)}, \quad p_i = \frac{1}{n}, \quad p_j = \frac{1}{n-1}, \quad \overline{p} = 0. \tag{3.18}$$

This is, in fact, the adaptation of Bird's direct simulation Monte Carlo (DSMC) method [1] to Eq. (1.1).

There are two main effects of a nonzero function γ.

First the collision partners w_i and w_j remain in the system, since only a part of their weights is transferred (cf. (3.8), (3.11)). If, in particular, $\kappa_1 > 0$, then all particles with velocities from A_ε will remain in the system losing a part of their weights during each collision (cf. (3.12)).

The second effect is on the distribution of the collision partners. Note that the probabilities (3.15), (3.16) do not depend on γ. Thus, the distribution of the partners in real collisions is determined by (3.17). If γ is large, i.e., close to its maximum value, $\max(\kappa_1, \kappa_2)$, then the collision is fictitious with small probability. Thus, a real collision between partners with large γ does occur more likely. If, in particular, $\kappa_2 > \kappa_1$, then collision partners w_i, $w_j \notin A_\varepsilon$ with $\tilde{w}_i$, $\tilde{w}_j \in A_\varepsilon$ will be favored in performing real collisions (cf. (3.12)).

The new parameters κ_1 and κ_2 allow us to modify the evolution of the particle system according to special numerical purposes. Thus, the method does not simply try to mimic the physical process. In this sense, it is a "non-DSMC" method.

TABLE I

$\kappa_1 = 1$, $\kappa_2 = 1$

n	N	$e_\varepsilon * 10^6$	$c_\varepsilon * 10^6$	$e_{m1} * 10^6$	$c_{m1} * 10^6$	m_{inc}	m_{rel}
16	640000	794	197/146	4040	555/652	1.7	3.63
32	320000	450	196/141	2137	554/630	1.8	3.52
64	160000	187	197/137	941	555/611	2.0	3.43
128	80000	107	197/134	493	553/595	2.1	3.36
256	40000	87	197/133	482	555/583	2.2	3.32
512	20000	145	197/131	443	558/579	2.2	3.31
1024	10000	130	195/131	217	553/578	2.2	3.28
10240	1000	55	198/130	410	547/580	2.2	3.28
102400	100	105	201/145	496	561/624	2.2	3.28

4. NUMERICAL EXPERIMENTS

In this section we present the results of numerical simulations according to the method described in the previous section. The method depends on the parameters κ_1, κ_2, ε via the function γ (cf. (3.12)) and on the parameter n (cf. (3.2)). We choose $\varepsilon = 0.01$ so that the specified region takes the form (cf. (3.10))

$$A_\varepsilon = A_{0.01} = [0.99, 1.). \tag{4.1}$$

We study the influence of the remaining parameters on the behavior of the particle system on the time interval [0, 1].

The main effect to be studied is the artificial increase of the number of particles in the region A_ε caused by the control parameters κ_1 and κ_2. However, it is important to clarify how this effect is related to other statistical properties of the system. To this end, we calculate the first moment of the solution of Eq. (1.1) (cf. (2.5)–(2.9))

$$M_1(t) = \int_0^1 uf(t, u)\, du \tag{4.2}$$

and the functional (cf. (2.10), (2.11))

$$F_\varepsilon(t) = \int_{0.99}^1 f(t, u)\, du. \tag{4.3}$$

4.1. *Some Statistical Notions*

First we introduce some definitions and notations that are important for the understanding of stochastic numerical schemes for kinetic equations.

The functionals to be calculated (4.2), (4.3) are of the form

$$F(t) = \int_0^1 \varphi(w) f(t, w)\, dw. \tag{4.4}$$

According to (3.3), a functional (4.4) is approximated by the random variable

$$\xi^{(n)}(t) = \int_0^1 \varphi(w)\mu^{(n)}(t, dw) = \sum_{i=1}^{m^{(n)}(t)} g_i^{(n)}(t)\varphi(w_i^{(n)}(t)). \tag{4.5}$$

In order to estimate and to reduce the random fluctuations of the estimator (4.5), a number N of independent ensembles of particles is generated. The corresponding values of the random variable are denoted by

$$\xi_1^{(n)}(t), ..., \xi_N^{(n)}(t).$$

The **empirical mean value** of the random variable (4.5),

TABLE II

$\kappa_1 = 1$, $\kappa_2 = 5$

n	N	$e_\varepsilon * 10^6$	$c_\varepsilon * 10^6$	$e_{m1} * 10^6$	$c_{m1} * 10^6$	m_{inc}	m_{rel}
16	640000	1177	196/97	3974	555/635	2.9	7.79
32	320000	604	197/91	1993	555/610	3.2	7.58
64	160000	249	197/87	1235	554/591	3.4	7.47
128	80000	178	197/84	428	553/580	3.6	7.41
256	40000	76	197/83	598	552/574	3.7	7.39
512	20000	81	196/83	299	550/565	3.7	7.37
1024	10000	44	197/82	338	553/562	3.7	7.38
10240	1000	76	197/82	449	560/573	3.7	7.36
102400	100	162	230/91	307	605/590	3.7	7.36

TABLE III

$\kappa_1 = 1$, $\kappa_2 = 10$

n	N	$e_\varepsilon * 10^6$	$c_\varepsilon * 10^6$	$e_{m1} * 10^6$	$c_{m1} * 10^6$	m_{inc}	m_{rel}
16	640000	1272	196/84	4585	555/629	4.9	11.9
32	320000	586	197/77	2060	556/607	5.3	11.5
64	160000	298	197/72	961	553/590	5.6	11.4
128	80000	167	197/69	816	556/579	5.8	11.4
256	40000	95	196/68	311	554/571	5.9	11.4
512	20000	82	197/67	289	553/566	5.9	11.4
1024	10000	51	196/68	571	561/571	5.9	11.4
10240	1000	38	199/67	473	554/540	6.0	11.4
102400	100	57	196/59	155	545/519	6.0	11.4

$$\eta_1^{(n,N)}(t) = \frac{1}{N}\sum_{j=1}^{N} \xi_j^{(n)}(t), \tag{4.6}$$

is then used as an approximation to the functional (4.4). The error of this approximation is

$$e^{(n,N)}(t) = |\eta_1^{(n,N)}(t) - F(t)| \tag{4.7}$$

containing the following two components:

The **systematic error** is the difference between the mathematical expectation of the random variable (4.5) and the exact value of the functional, i.e.,

$$e_{\text{sys}}^{(n)}(t) = E\xi^{(n)}(t) - F(t). \tag{4.8}$$

The **statistical error** is the difference between the empirical mean value and the expected value of the random variable, i.e.,

$$e_{\text{stat}}^{(n,N)}(t) = \eta_1^{(n,N)}(t) - E\xi^{(n)}(t).$$

A **confidence interval** for the expectation of the random variable $\xi^{(n)}(t)$ is obtained as

$$I_p = \left[\eta_1^{(n,N)}(t) - \lambda_p \sqrt{\frac{\text{Var}\ \xi^{(n)}(t)}{N}}, \eta_1^{(n,N)}(t) + \lambda_p \sqrt{\frac{\text{Var}\ \xi^{(n)}(t)}{N}}\right], \tag{4.9}$$

where

$$\text{Var}\ \xi^{(n)}(t) := E[\xi^{(n)}(t) - E\xi^{(n)}(t)]^2 = E[\xi^{(n)}(t)]^2 - [E\xi^{(n)}(t)]^2 \tag{4.10}$$

is the **variance** of the random variable (4.5) and $p \in (0, 1)$ is the **confidence level**. It means that

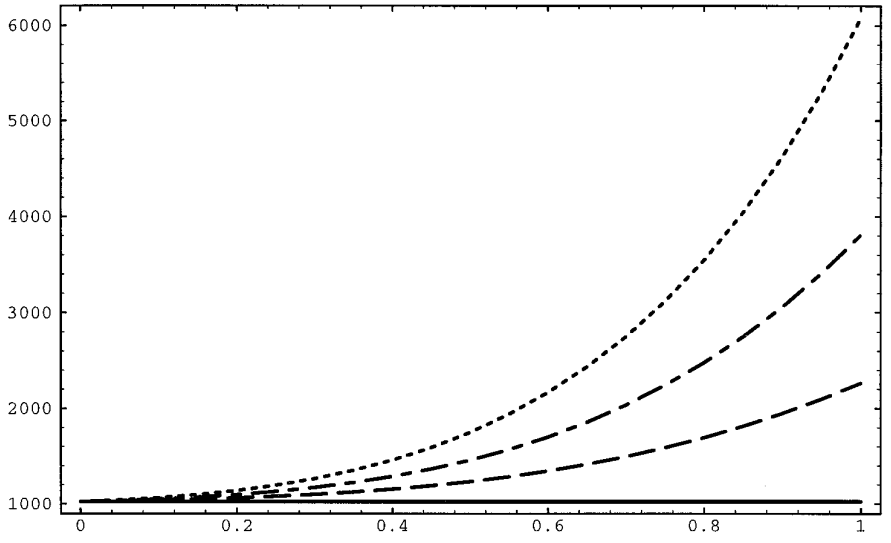

FIG. 1. Number of particles $m(t)$.

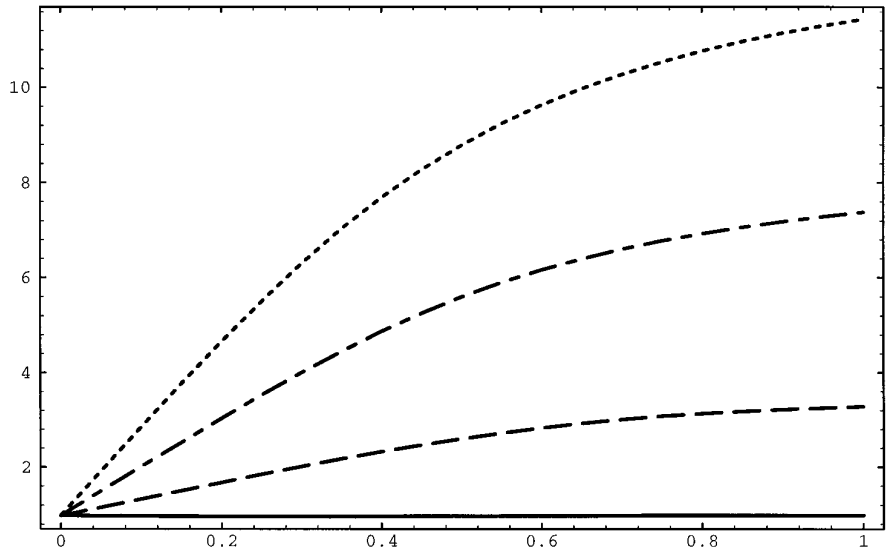

FIG. 2. Percentage of particles $m_{\text{rel}}(t)$ in the region A_ε.

$$\text{Prob}\{E\xi^{(n)}(t) \notin I_p\} = \text{Prob}\left\{|e_{\text{stat}}^{(n,N)}(t)| \geq \lambda_p \sqrt{\frac{\text{Var } \xi^{(n)}(t)}{N}}\right\} 1 - p.$$

Thus, the value

$$c^{(n,N)}(t) = \lambda_p \sqrt{\frac{\text{Var } \xi^{(n)}(t)}{N}} \tag{4.11}$$

is a probabilistic upper bound for the statistical error.

In the calculations, we use a confidence level of $p = 0.999$ and $\lambda_p = 3.2$. The variance is approximated by the corresponding empirical value (cf. (4.10)); i.e.,

$$\text{Var } \xi^{(n)}(t) \sim \eta_2^{(n,N)}(t) - [\eta_1^{(n,N)}(t)]^2,$$

where

$$\eta_2^{(n,N)}(t) = \frac{1}{N}\sum_{j=1}^{N} [\xi_j^{(n)}(t)]^2,$$

is the **empirical second moment** of the random variable (4.5).

4.2. *Influence of the Control Parameters*

We perform the calculations for different combinations of the parameters κ_1 and κ_2. The initial distribution $f_0(v)$ is approximated according to (3.5), and the random time counter (3.14) is used. A rather complete set of numerical results is given in Tables I–III, where the following notations are used.

The supremum over the time interval $[0, 1]$ of the error (4.7) is denoted by e_{m1} and e_ε for the functionals (4.2) and (4.3), respectively. The statistical error bound (4.11) is displayed both at the beginning and the end of the time interval $[0, 1]$, and is denoted by c_{m1} and c_ε for the functionals (4.2) and (4.3), respectively.

Finally, the increase factor for the number of particles in the system

$$m_{\text{inc}}(t) = \frac{m(t)}{m(0)} = \frac{m(t)}{n} \tag{4.12}$$

and the percentage of particles in the region A_ε

$$m_{\text{rel}}(t) = \frac{\sum_{i=1}^{m(t)} \P_{A_\varepsilon}(w_i(t))}{m(t)} \tag{4.13}$$

at $t = 1$ are denoted by m_{inc} and m_{rel}, respectively.

TABLE IV

n	N	$e_{\text{det}} * 10^6$	$c_{\text{det}} * 10^6$	$e_{\text{sto}} * 10^6$	$c_{\text{sto}} * 10^6$
4	2560000	72878	714	17003	718
8	1280000	28754	712	7873	710
16	640000	15298	706	3902	705
32	320000	5256	702	2269	703
64	160000	2354	702	498	701
128	80000	1692	700	1085	703
256	40000	755	702	337	702
512	20000	505	700	359	696
1024	10000	347	711	308	706

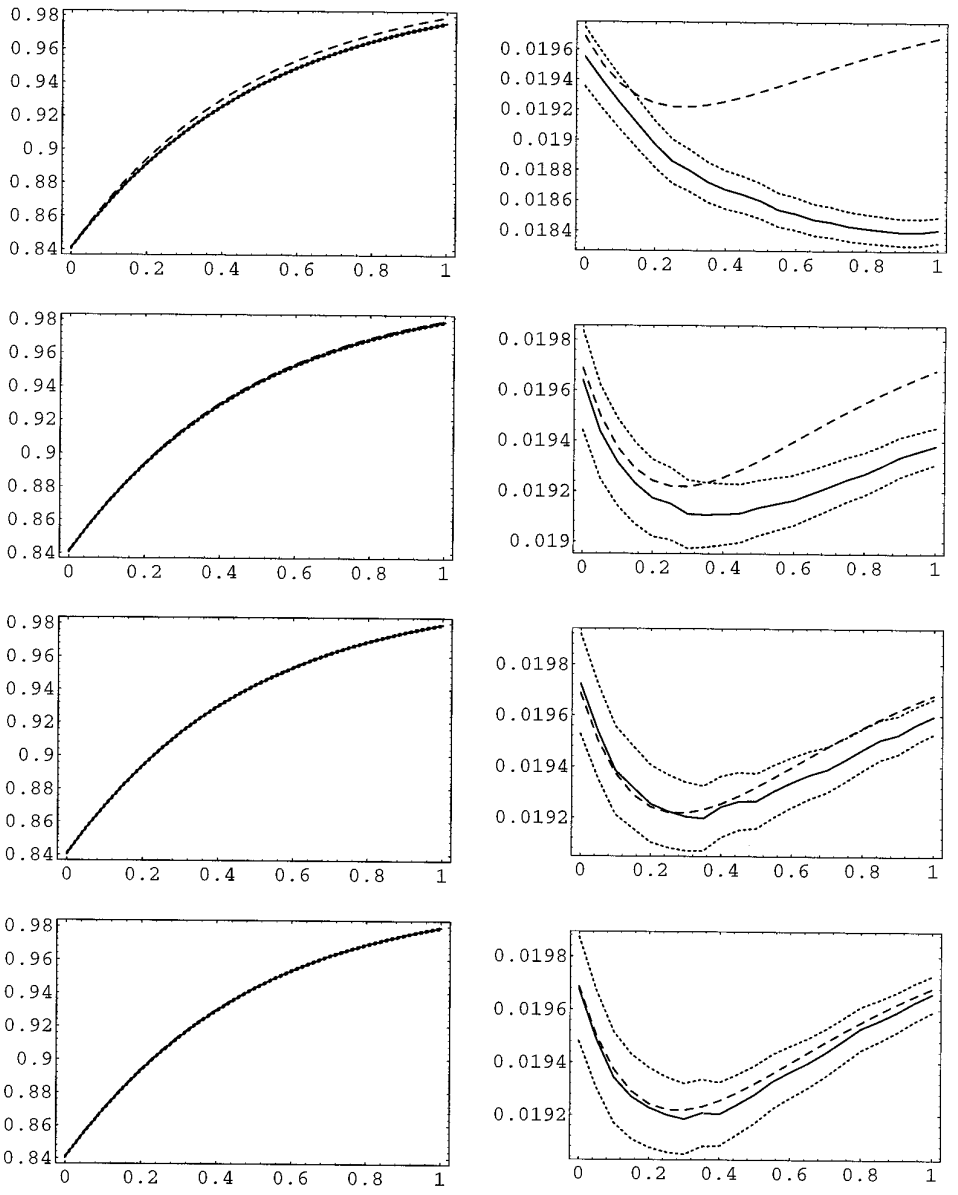

FIG. 3. Method with $\kappa_1 = 1$, $\kappa_2 = 10$ and $n = 16, 64, 256, 1024$ (from above).

The numerical material contained in Tables I–III allows us to study the influence of the parameters κ_1, κ_2, and n on three characteristic properties of the method—the number of particles in the prescribed region A_ε, the systematic error (4.8), and the bound for the statistical error (4.11).

The increase factor for the **number of particles** in the system (4.12) as well as the percentage of particles in the region A_ε (4.13) become independent of n for sufficiently large n. Figures 1 and 2 show the time dependent behavior of $m(t)$ and $m_{\text{rel}}(t)$ for $n = 1024$ and $N = 10{,}000$. The different lines correspond to $\kappa_1 = 1$, $\kappa_2 = 1$ (dashed), $\kappa_1 = 1$, $\kappa_2 = 5$ (dashed-dotted), and $\kappa_1 = 1$, $\kappa_2 = 10$ (dotted). For comparison, the corresponding values for the standard method ($\kappa_1 = 0$, $\kappa_2 = 0$) are displayed by a solid line.

From the knowledge of the behavior of the error (4.7), it is possible to draw some conclusions about the behavior of the **systematic error** (4.8), while the error (4.7) is large compared with the statistical error bound (4.11). Thus, it can be seen from the numerical results in Tables I–III that the systematic error behaves roughly like $O(n^{-1})$.

Figure 3 shows the time-dependent behavior of certain relevant quantities for the method with $\kappa_1 = 1$, $\kappa_2 = 10$. The left-hand side of the figure corresponds to the first

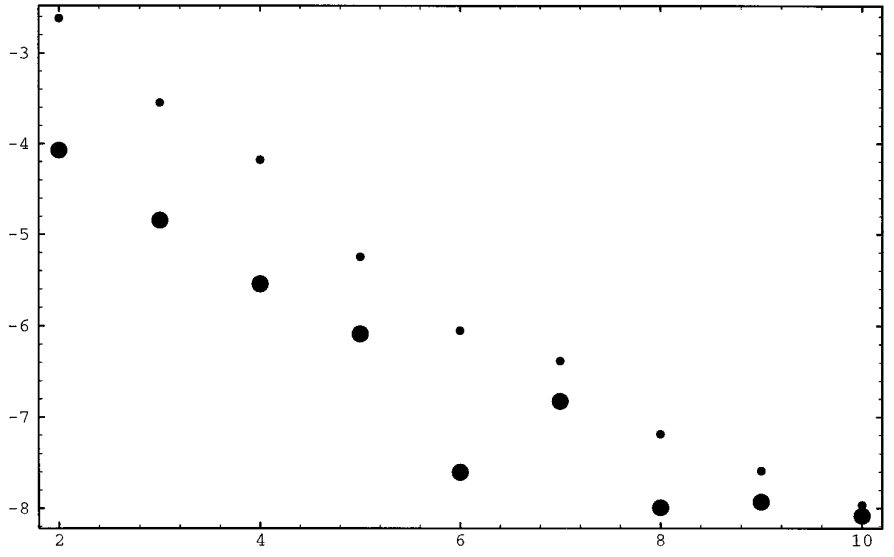

FIG. 4. Dependence on n of the error for different time counters.

moment (4.2), while the right-hand side corresponds to the functional (4.3). The exact values of the functionals as functions of time are represented by the dashed lines. The computed empirical mean values (4.6) are displayed by solid lines, and the corresponding confidence intervals (cf. (4.9)) by dotted lines.

Note that the exact values to be approximated are $F_\varepsilon(1) = 0.019680$ and $M_1(1) = 0.979422$. Consequently, an error 0.000197 is of the order of 1% for the functional F_ε, and an error 0.000555 is of the order of 0.05% for the first moment.

The behavior of the **statistical error bound** (4.11) is determined by the variance (4.10) of the random variable (4.5). Concerning the behavior of the variance there are two main observations based on the numerical data of Tables I–III.

First, the statistical error bound c remains constant when the product nN is fixed. According to (4.11), one obtains

$$\frac{\operatorname{Var} \xi^{(n)}(t)}{N} \approx \text{const.}$$

This indicates a behavior like

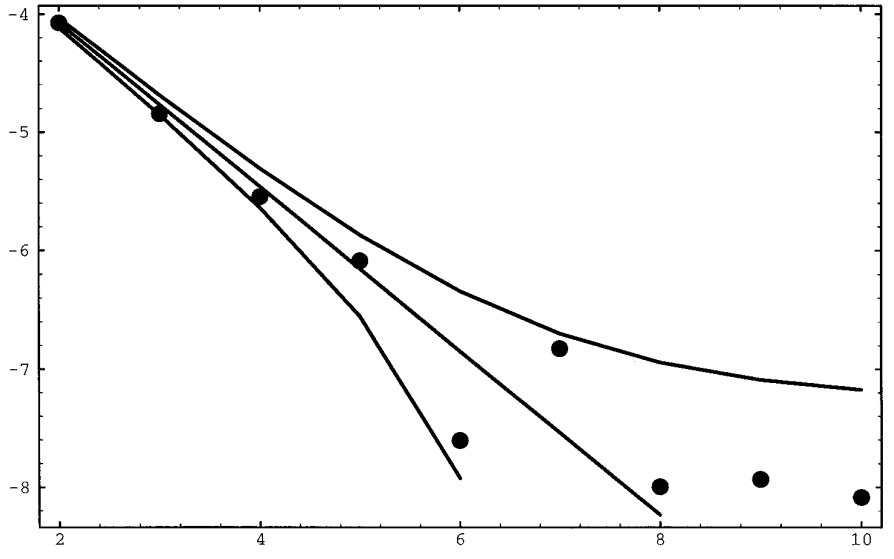

FIG. 5. Error for the stochastic time counter with confidence intervals.

TABLE V

i-method	n_I	$e_{\text{beg}} * 10^6$	$e_{\text{sup}} * 10^6$	$c_{\text{beg}} * 10^6$	$c_{\text{end}} * 10^6$
1	1	140	308	554	706
1	2	97	224	317	697
1	4	52	361	156	701
1	8	27	313	78	699
1	16	14	248	38	699
1	32	7	243	19	694
1	1024	0	261	0	695
2	1	0	572	0	698

TABLE VI

κ_1	κ_2	n_I	$e_{\text{beg}} * 10^6$	$e_{\text{sup}} * 10^6$	$c_{\text{beg}} * 10^6$	$c_{\text{end}} * 10^6$
0.	0.	1	83	129	196	240
0.	0.	2	117	157	193	239
0.	0.	4	21	143	193	239
0.	0.	8	8	113	189	239
0.	0.	16	45	81	181	241
0.	0.	32	40	119	162	237
0.	0.	1024	13	131	16	236
1.	5.	1	25	44	197	82
1.	5.	1024	1	27	16	77

$$\text{Var } \xi^{(n)}(t) = O(n^{-1}).$$

Second, there is a reduction in the variance of the estimator for the functional F_ε, for appropriate parameters κ_1 and κ_2. The statistical error bound c_ε decreases from about 134 for $\kappa_2 = 1$ to about 67 for $\kappa_2 = 10$, i.e., by a factor of 2. This effect is only partly caused by the increase in the number of particles in the system, which gives a factor of about $\sqrt{3}$. Another reason is the increased relative number of particles in the region A_ε. A more significant variance reduction (especially compared with the standard method) is achieved when ε is smaller (cf. [9] concerning the case $\varepsilon = 0.0001$).

4.3. *Time Counter*

Here we study the influence of the choice of the time counter on the behavior of the system. To this end, we calculate the first moment (4.2) with the standard method ($\kappa_1 = 0$, $\kappa_2 = 0$) and both the deterministic time counter (3.13) and the stochastic time counter (3.14). The initial distribution $f_0(v)$ is approximated according to (3.5).

The numerical results are given in Table IV. The supremum over the time interval [0, 1] of the error (4.7) is denoted by e_{det} and e_{sto} for the time counters (3.13) and (3.14), respectively. The statistical error bound (4.11) at the end of the time interval is denoted by c_{det} and c_{sto}, respectively.

The systematic error behaves roughly like $O(n^{-1})$ (cf. the corresponding comments in the previous subsection). The errors for both time counters are displayed in Fig. 4 in a logarithmic scale dependent on n. Note that the random deviations from a linear behavior are within the confidence intervals, as Fig. 5 shows.

4.4. *Initial Approximation*

Here we study the influence of the approximation of the initial value on the behavior of the system. The stochastic time counter (3.14) is used. The initial number of particles is $n = 1024$ and the number of repetitions is $N = 10{,}000$. The behavior of the statistical error bound (4.11) is studied for different values of n_I (cf. (3.6)).

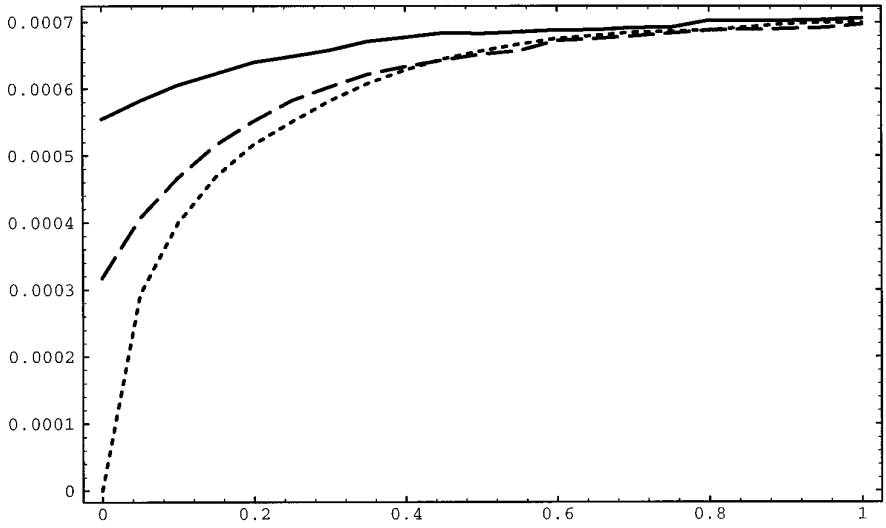

FIG. 6. Statistical error bounds for the first moment (4.2).

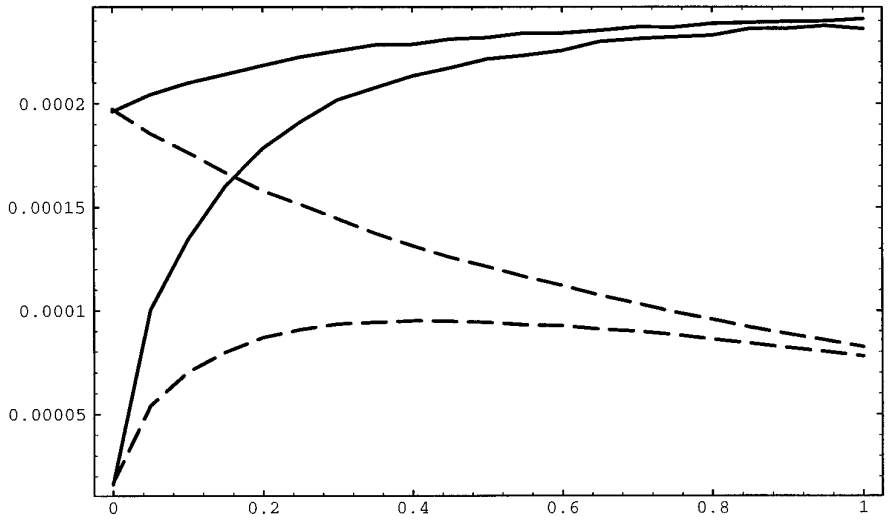

FIG. 7. Statistical error bounds for the functional (4.3).

First we calculate the first moment (4.2) with the standard method ($\kappa_1 = \kappa_2 = 0$). The numerical results are given in Table V. Here e_{beg} denotes the error (4.7) at $t = 0$, e_{sup} is the supremum of the error over the time interval $[0, 1]$, while c_{beg} and c_{end} denote the statistical error bound at $t = 0$ and $t = 1$, respectively. Either pseudo-random numbers (i-method = 1) or a low discrepancy sequence (i-method = 2) were used in (3.6).

The time dependent behavior of the statistical error bound is shown in Fig. 6. The solid line in this figure represents the values for $n_I = 1$. The dashed line represents the results for $n_I = 2$ and the dotted line for the low discrepancy sequence. The lines for $n_I = 4, 8, \ldots$ are between the dashed and the dotted lines and we decided not to plot them in order not to overload the figure. The line for $n_I = 1024$ coincides with the line for the low discrepancy sequence.

Figure 6 shows that the reduction of the statistical error bound and, correspondingly, of the variance, which can be achieved by a better approximation of the initial function $f_0(u)$, remains remarkable for some time after the start of the computations. But if we are interested in computing the steady-state solution of the problem then we will obtain nearly the same quality of the stochastic solution, even if we do not care so much about the approximation of the initial function.

Next we calculate the functional (4.3) using the method with the parameters $\kappa_1 = \kappa_2 = 0$ and $\kappa_1 = 1$, $\kappa_2 = 5$. The results are contained in Table VI. As before, e_{beg}, e_{sup} denote the systematic error at $t = 0$ and the supremum of the systematic error over the time interval [0, 1], and c_{beg}, c_{end} denote the statistical error bound (4.11) at $t = 0$ and $t = 1$, respectively.

Figure 7 shows the time dependent behavior of the statistical error bound for both methods. The solid lines represent the results for $\kappa_1 = 0$, $\kappa_2 = 0$, while the dashed lines correspond to $\kappa_1 = 1$, $\kappa_2 = 5$.

The approximation of the initial function corresponding to $n_I = 1024$ is much better if we compute the solution for only a short time. However, again the asymptotic behavior of both methods does not depend on the approximation of the initial distribution.

5. CONCLUSIONS

We studied a stochastic weighted particle method based on a generalized mechanism of modelling collisions between particles.

The main feature of the new method is the presence of certain control parameters giving the opportunity to adapt the behavior of the particle system to specific numerical purposes. It was shown that the relative number of particles with prescribed velocities may be artificially increased, while other macroscopic quantities like moments are still computed correctly.

The computations were performed for a model kinetic equation, for which the exact solution is known, since in this case it was possible to separate various numerical effects. However, the results indicate how to proceed in the case of more realistic kinetic equations, like the spatially inhomogeneous Boltzmann equation.

In some cells of the physical space, one may define appropriate sets of velocities directed into regions, where macroscopic quantities cannot be computed sufficiently accurately due to a low particle density. During the collision simulation step the control parameters of the method are used to increase the number of particles with prescribed velocities. These particles will finally reach the desired

region, creating there a better statistics than the direct simulation method.

REFERENCES

1. G. A. Bird, *Molecular Gas Dynamics and the Direct Simulation of Gas Flows* (Clarendon Press, Oxford, 1994).
2. A. Bobylev and S. Rjasanow, preprint, Keldysh Institute for Applied Mathematics, Moscow, 1996, to appear.
3. C. Cercignani, R. Illner, and M. Pulvirenti, *The Mathematical Theory of Dilute Gases* (Springer-Verlag, New York, 1994).
4. R. Illner and S. Rjasanow, *European J. Mech. B Fluids* **13**(2), 197 (1994).
5. R. Illner and W. Wagner, *J. Statist. Phys.* **70**(3/4), 773 (1993).
6. M. S. Ivanov and S. V. Rogazinskij, *Soviet J. Numer. Anal. Math. Modelling* **3**(6), 453 (1988).
7. H. Neunzert, F. Gropengiesser, and J. Struckmeier, ''Computational Methods for the Boltzmann Equation,'' *Applied and Industrial Mathematics,* edited by R. Spigler (Kluwer Academic, Dordrecht, 1991), p. 111.
8. S. Rjasanow and W. Wagner, *J. Comput. Phys.* **124**(2), 243 (1996).
9. S. Rjasanow and W. Wagner, preprint No. 157, Weierstrass Institute for Applied Analysis and Stochastics, Berlin, 1995; *Comput. Math. Appl., 1996,* to appear.